Critical heat flux around strongly heated nanoparticles

Samy Merabia,[1,*] Pawel Keblinski,[2] Laurent Joly,[1] Laurent J. Lewis,[3] and Jean-Louis Barrat[1]
[1]*Université de Lyon, Université de Lyon I, Laboratoire de Physique de la Matière Condensée et des Nanostructures, CNRS, UMR 5586, 43 Boulevard du 11 Nov. 1918, 69622 Villeurbanne Cedex, France*
[2]*Materials Science and Engineering Department, Rensselaer Polytechnic Institute, Troy, New York 12180, USA*
[3]*Département de Physique, Université de Montréal, Case Postale 6128, Succursale Centre-Ville, Montréal, Québec H3C 3J7, Canada*
(Received 21 August 2008; published 10 February 2009)

We study heat transfer from a heated nanoparticle into surrounding fluid using molecular dynamics simulations. We show that the fluid next to the nanoparticle can be heated well above its boiling point without a phase change. Under increasing nanoparticle temperature, the heat flux saturates, which is in sharp contrast with the case of flat interfaces, where a critical heat flux is observed followed by development of a vapor layer and heat flux drop. These differences in heat transfer are explained by the curvature-induced pressure close to the nanoparticle, which inhibits boiling. When the nanoparticle temperature is much larger than the critical fluid temperature, a very large temperature gradient develops, resulting in close to ambient temperature just a radius away from the particle surface. The behavior reported allows us to interpret recent experiments where nanoparticles can be heated up to the melting point, without observing boiling of the surrounding liquid.

DOI: 10.1103/PhysRevE.79.021404 PACS number(s): 82.70.−y, 65.80.+n, 44.35.+c, 68.08.De

Sub-micron-scale heat transfer is attracting a growing interest [1], motivated by both fundamental and technological issues. The fast emergence of this field is, to a large extent, associated with the development of micro- and nanotechnologies. In some cases, thermal transfer is part of the system function (e.g., the use of nanofluids for heat transport or of multilayered materials for thermal insulation). In other cases, the enhancement of heat transfer is a key to a proper operation of the microsystem (e.g., microprocessors) and involves integration on ever smaller scales of devices such as microheat pipes. Although these systems are of micrometer size, the regions that limit heat transfer—interfaces, constrictions—are often characterized by even smaller lengths, bringing heat transfer issues into the domain of nanosciences. Recent interest in heat transport around nanoparticles has arisen in part from the particular properties of the so-called "nanofluids" [2,3]—i.e., colloidal suspensions of solid nanoparticles—which exhibit improved thermal transport properties. On the fundamental side, a number of laser-heating studies were performed, demonstrating even melting of metal nanoparticles without macroscopic boiling of the embedding liquid [4,5]. The physics of this phenomenon involves a complex interplay between boiling, heat transfer, and particle-fluid interactions (wetting) and is still poorly understood.

In this article, we use molecular dynamics (MD) simulation to study heat transfer around a nanoparticle surrounded by a volatile fluid. We characterize heat transfer in situations where the nanoparticle is heated above the fluid boiling point and/or critical temperature, and compare this situation to the case of flat interfaces. We show that the fluid around nanoparticle can sustain large heat fluxes, well above the critical heat flux of the bare fluid on a flat interface. Accompanying the large heat flux are extreme temperature gradients, allowing for localization of the hot liquid to volumes comparable with nanoparticle size.

*smerabia@gmail.com

MD has been already applied successfully to characterize heat transfer across a nanoparticle-fluid interface in the absence of fluid phase change [6–8]. This technique has the advantage of giving local detailed information on heat transfer and on the structure of the fluid close to the nanoparticle interface as well. Furthermore, the system at hand is perfectly controlled, which allows one to pinpoint unambiguously the relevant physical mechanisms at work.

The model we simulate consists of a solid nanoparticle made of 555 atoms immersed in a fluid of 23 000 atoms. All atoms interact through a Lennard-Jones potential $V_{\alpha\beta}(r)=4\epsilon[(\sigma/r)^{12}-c_{\alpha\beta}(\sigma/r)^{6}]$, where α and β refer to solid or liquid atoms. The potential has a cutoff radius 2.5σ where σ is the diameter of the atoms. The parameters ϵ and σ are taken to be the same for both phases. The parameter $c_{\alpha\beta}=1$ if $\alpha=\beta$; $c_{\alpha\beta}=c$ otherwise, where c controls the wetting interaction between the fluid and solid nanoparticles. In this work, we shall consider three cases: $c=0.5$ and 1, which correspond, respectively, to solvophobic and solvophilic interactions, and $c=2$, which describes strong bonding between the solid and the fluid. The solid nanoparticle is obtained from a spherical cut of an equilibrium fcc lattice. In addition to the Lennard-Jones interactions, atoms inside the particles are connected to their neighbors with FENE springs [7] $V(r)=-0.5kR_0^2\ln[1-(r/R_0)^2]$, with $k=30\epsilon/\sigma^2$ and $R_0=1.5\sigma$. This nearest-neighbor bonding allows one to heat up the nanoparticle without observing melting or fragmentation. This simple modeling is intended to mimic the situation of metallic or oxide nanoparticles, with rather high cohesive energies, in volatile organic solvents with much lower cohesion and a low boiling temperature.

Throughout, lengths, energies, and times are expressed in units of σ, ϵ, and $\tau=\sqrt{m\sigma^2/\epsilon}$, where m denotes the common mass of the atoms. For liquid argon, the corresponding values are $\sigma=0.3$ nm, $\epsilon=0.025$ eV, and $\tau\simeq 1$ ps. We integrate the equations of motion using a velocity Verlet algorithm with a time step $dt=0.005\tau$. All systems considered have been first equilibrated at a constant temperature $T_0=0.75$ un-

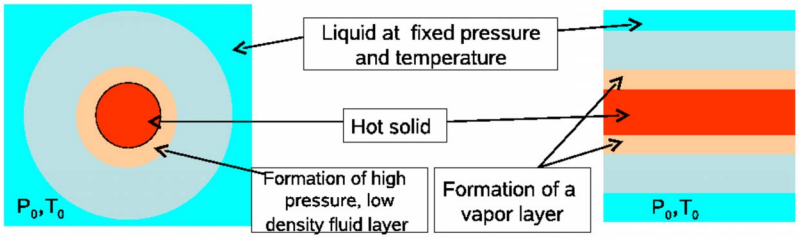

FIG. 1. (Color online) Schematic illustration of the simulation setup for the nanoparticle and planar cases.

der constant pressure $P_0=0.015$ (using a Nose-Hoover temperature thermostat and pressure barostat [9]). The temperature T_0 is below the boiling temperature, which we found to be $T_b \simeq 0.8$, using independent simulations of a liquid-vapor interface, under the pressure P_0 we are working at. After 100 000 time steps of equilibration, the nanoparticle is heated up at different temperatures $T_p > T_b$ by rescaling the velocities of the solid particles at each time step, while the whole system is kept at the constant pressure P_0 using a NPH barostat. The fluid beyond a distance 10σ from the particle surface is thermostatted at $T_0=0.75$, again using velocity rescaling. A global setup of the system is depicted in Fig. 1. Temperature, density, and pressure fields have been obtained by averaging the corresponding quantities during 100 000 time steps in nanoparticle-centered spherical shells of width $\simeq 0.15\sigma$, after a steady state is reached. The Irving-Kirkwood formula [10] is used to calculate the normal component of the pressure tensor P_{rr}. Finally, we calculate the heat flux density flowing through the solid particle by measuring the power supply needed to keep the nanoparticle at the target temperature T_p.

Figure 2 displays steady-state temperature profiles close to the nanoparticle surface for different temperatures T_p of the nanoparticle. For low T_p, the temperature field in the liquid is practically indistinguishable from the form $A/r+B$, predicted by continuum heat transfer equations in homogenous media in spherical geometry. Inside the solid, the temperature is not uniform, but slightly curved downwards, due to the finite conductivity of the nanoparticle. Noticeably, the

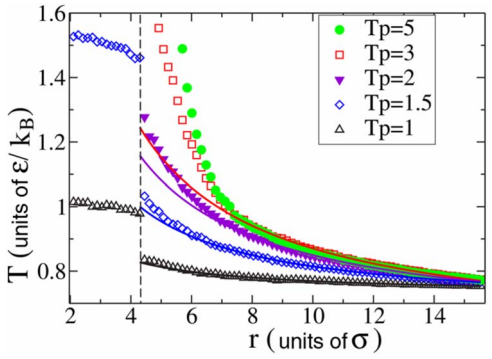

FIG. 2. (Color online) Steady-state temperature field across the liquid-nanoparticle interface, obtained with molecular dynamics. The nanoparticle-fluid interaction is hydrophilic ($c=1$). The position of the nanoparticle surface is indicated by dashed lines, r measuring the distance to the center of the nanoparticle. Solid curves correspond to fits by the continuum theory result $T(r)=A/r+B$. Note that for $T_p=1$, the solid curve is indistinguishable from the simulation data.

temperature is not continuous at the solid interface. The corresponding temperature jump ΔT is related to the existence of a finite interfacial resistance $R=\Delta T/j$, j being the flux density flowing through the interface. This effect is well known since the pioneering work of Kapitza on helium and is particularly important when the dimensions of the system considered are comparable to the Kapitza length $l_K=\lambda R$, λ denoting the thermal conductivity of the liquid [11]. For the usual liquids, l_K is on the order of a few nm [12,13]; thus, the effects are particularly important for heat transfer around nanoparticles. From Fig. 2, we measured a value $R \simeq 1.6$, which is consistent with previous MD simulations [7,14] and consistent with the experimental determinations [13,15] in the case of hydrophilic interactions, considering that a value of $R=1$ in our units corresponds to an interfacial resistance on the order of 0.1 K m^2 MW^{-1}. For solvophobic interactions, we have measured a larger interfacial resistance ($R=12$ for $c=0.5$), while for $c=2$, no temperature jump is seen due to very good thermal contact between the nanoparticle and the fluid. Upon increasing the temperature of the nanoparticle, deviations from the $1/r$ behavior are clearly seen in Fig. 2 when the local temperature exceeds $T \simeq 1$, which is about equal to the critical fluid temperature. Interestingly, the temperature profile steepens close to the nanoparticle surface, corresponding to a decrease of the local effective conductivity, and providing a "thermal shield" for the fluid away from the particle surface at distances of one particle radius. This thermal barrier indicates that the particle can be heated to very large temperatures, while the liquid at a particle diameter away from the surface can have close to ambient temperature. Also the temperature gradient at the particle surface can reach enormous values 0.3 in reduced units (see Fig. 2), which translates to 300 K/nm for argon parameters. To relate these features to possible structural changes of the fluid, we have considered the density profile around the nanoparticle in Fig. 3. When heating is moderate, some layering is present, reminiscent of the layering observed at a hydrophilic interface in the absence of heating. When the temperature of the particle increases, the height of the first peak decreases, while layering becomes blurred, and a dilute layer appears. Note, however, that the corresponding density within this layer is still one order of magnitude larger than the vapor density at coexistence, which we determined using independent simulations of a stable liquid-vapor interface. Correspondingly, the inset of Fig. 3 shows a gradual increase of the normal pressure in the vicinity of the particle, with values of the pressure approaching the critical pressure, estimated to be $P_c=0.1$ [16]. This increase in the local pressure, which is similar to a Laplace pressure effect in capillarity, appears to prevent the formation of a vapor. It is also worth noting that the decrease of density is accompanied by

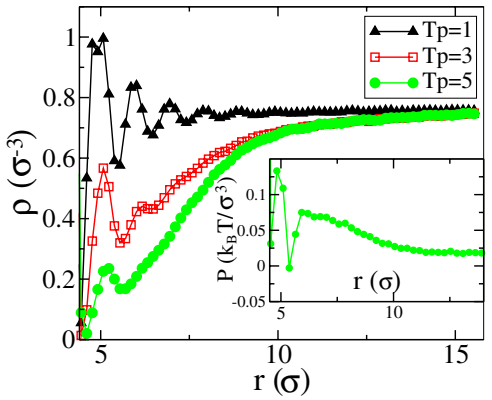

FIG. 3. (Color online) Density profile close to a hot nanoparticle having a temperature T_p. The inset displays the normal pressure close to the hottest nanoparticle (T_p=5).

the existence of a limiting temperature profile far away from the particle, as seen in Fig. 2. It is interesting to contrast this situation with the one obtained in a planar geometry. To this end, we performed a set of simulations in which a fcc solid slab cut along the 100 direction is in contact on both sides with the fluid. The system is periodic in all directions, and both the solid slab and the liquid at a distance 12σ from the solid are thermostatted at T=0.75. The system is kept at constant pressure P_0=0.015 in the direction normal to the solid slab. After equilibration, the temperature of the solid slab is raised in order to establish a heat flux between the solid and the bulk liquid. The two situations (nanoparticle and flat solid) are compared in Fig. 4 in terms of the heat flux density as a function of the temperature of the solid. In each case, the three different wetting conditions (c=0.5,1,2) are considered. The difference between the nanoparticle case and that of a flat solid is striking. For the nanoparticle, two regimes can be distinguished, depending on the heating intensity. For low temperatures, the flux increases linearly with T_p up to a kink temperature T_k. The initial slope increases as the wetting becomes better, while the kink temperature T_k moves to higher values with increasing the solvophobic character of the particle. Beyond T_k the flux levels off at a plateau value which increases with the wetting parameter c. Interestingly,

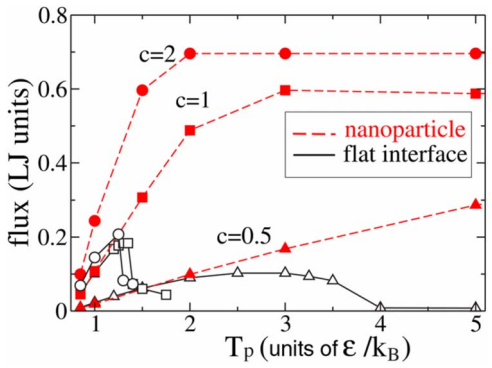

FIG. 4. (Color online) Flux density as a function of the temperature of a nanoparticle (solid symbols) compared to the flux density flowing through a flat interface (open symbols). Lines are guides to the eye.

the transition between these two behaviors takes place when deviations from the $1/r$ profile become significant and the liquid density of the first peak close to the particle decreases significantly. This confirms that the nature of the fluid in the interfacial zone is modified significantly for such heat fluxes, with a decreased conductivity—or equivalently a high value of the effective interfacial resistance. For flat interfaces, on the other hand, a quite different scenario appears: for low fluxes, the flux increases nearly linearly with temperature and the curves are practically indistinguishable from their nanoparticle counterparts. However, the heat flux density drops abruptly when the temperature is raised above a critical temperature that increases with hydrophobicity. The corresponding maximum heat flux increases with wetting. This maximum in the heat flux can be described as a "critical heat flux" [17] phenomenon, observed here at the atomic scale. Note also that this drop occurs below the kink temperature T_k, but still beyond the boiling temperature T_b=0.8.

From a microscopic standpoint, the drop in the heat flux is associated with the formation of a vapor layer and a nonequilibrium drying of the surface. Note that nonequilibrium drying of the surface has also been observed with MD [18].

Due to its low conductivity, this vapor layer completely blocks heat transfer from the solid. The density within the flat vapor layer is $\simeq$0.02, one order of magnitude smaller than the dilute fluid layer surrounding hot nanoparticles. Furthermore, the pressure within this layer is uniform and equal to the imposed pressure P_0. This is in contrast with the nanoparticle case, where the local curvature of the iso-density curves imposes an increase in the pressure and in turn prevents the formation of a well defined vapor layer. In spite of this difference, a critical heat flux can be defined both for the nanoparticle and for the planar walls. Any attempt to transfer a flux density higher than the limiting values shown in Fig. 4 would result in an unbounded increase of the temperature of the nanoparticle and eventually to its destruction. The critical heat flux, however, is increased by a factor of almost 4 compared to the planar case.

Many experiments that probe heat transfer at the nanoscale are based on time-resolved studies of heat transfer in a transient, rather than stationary, regime. We therefore consider the influence of the critical heat flux on the behavior observed in such experiments. Our simulation of the transient regime proceeds by switching off the heating of the nanoparticle and monitoring the cooling process into the thermostatted fluid. Figure 5 displays the cooling kinetics of particles, starting from various initial temperatures T_p. Two behaviors are to be distinguished. When T_p is smaller than the kink temperature T_k discussed before (i.e., the initial flux is smaller than critical), the relaxation is typically exponential and the interfacial resistance extracted from fitting the relaxation curves [7] is in good agreement with the value found from the steady-state temperature profiles. On the other hand, when T_p exceeds T_k, the relaxation is no longer exponential but initially linear, which corresponds to a constant heat flux flowing through the interface. This early relaxation is followed by a second step, where the decay is more exponential, with a decay time typically 20% smaller than the value reported for lower initial temperature. Hence, the change of behavior revealed by our simulations and the

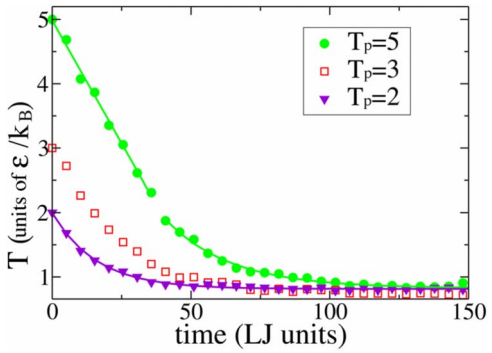

FIG. 5. (Color online) Cooling kinetics for a wetting nanoparticle ($c=1$) after a steady state was reached, where the particle's temperature was maintained fixed at a temperature T_p.

existence of a critical heat flux around nanoparticles could be assessed experimentally by monitoring the cooling kinetics in pump-probe experiments.

In summary, we have investigated heat transfer from nanoparticles and planar interfaces using molecular simulations under conditions of high flux and close to the boiling transition of the carrier fluid. In both cases the existence of a critical heat flux, above which heat transfer is impossible, is observed. This heat flux is considerably higher in the case of nanoparticles, as the formation of a blocking vapor layer is prevented by the increased pressure around the nanoparticle. This suggests that nanoparticles could be heated to rather high temperatures inside the host fluid. The existence of the critical heat flux would manifest itself by a change of regime in the transient absorption experiments under high-flux and high-temperature conditions [4]. Our study also suggests that nanoscale features could significantly modify the heat transfer properties of solid surfaces in this regime.

All the simulations were done using the MD code LAMMPS (http://www.cs.sandria.gov sjplimp/lammps.html). This work is supported by the Grant "Opthermal" from Agence Nationale de la Recherche, as well as grants from the Natural Sciences and Engineering Research Council of Canada (NSERC) and the *Fonds Québécois de la Recherche sur la Nature et les Technologies* (FQRNT). We thank the *Réseau Québécois de Calcul de Haute Performance* (RQCHP) for computer resources.

[1] D. G. Cahill *et al.*, J. Appl. Phys. **93**, 793 (2003).
[2] J. A. Eastman, S. R. Phillpot, S. U. S. Choi, and P. Keblinski, Annu. Rev. Mater. Res. **34**, 219 (2004).
[3] X. Q. Wang and A. S. Mujumdar, Int. J. Therm. Sci. **46**, 1 (2007).
[4] M. Hu, P. Hristina, and G. V. Hartland, Chem. Phys. Lett. **391**, 220 (2004).
[5] A. Plech, V. Kotaidis, S. Grésillon, C. Dahmen, and G. von Plessen, Phys. Rev. B **70**, 195423 (2004).
[6] M. Vladkov and J. L. Barrat, J. Comput. Theor. Nanosci. **5**, 187 (2008).
[7] M. Vladkov and J. L. Barrat, Nano Lett. **6**, 1224 (2006).
[8] W. Evans, J. Fish, and P. Keblinski, Appl. Phys. Lett. **88**, 093116 (2006).
[9] D. Frenkel and B. Smit, *Understanding Molecular Simulation* (Academic, San Diego, 1996).
[10] F. Varnik, J. Baschnagel, and K. Binder, J. Chem. Phys. **113**, 4444 (2000).
[11] J. L. Barrat and F. Chiaruttini, Mol. Phys. **101**, 1605 (2003).
[12] L. Xue, P. Keblinski, S. R. Phillpot, S. U.-S. Choi, and J. A. Eastman, J. Chem. Phys. **118**, 337 (2003).
[13] Z. Ge, D. G. Cahill, and P. V. Braun, Phys. Rev. Lett. **96**, 186101 (2006).
[14] The interfacial resistance that we measured is larger than the value reported in [7] due to the low pressure we are working at.
[15] O. M. Wilson, X. Hu, D. G. Cahill, and P. V. Braun, Phys. Rev. B **66**, 224301 (2002).
[16] A. Trokhymchuk and J. Alejandre, J. Chem. Phys. **111**, 8510 (1999).
[17] P. G. Debenedetti, *Metastable Liquids: Concepts and Principles* (Princeton University Press, Princeton, 1996).
[18] P. Yi, D. Poulikakos, J. Walther, and G. Yadigaroglu, Int. J. Heat Mass Transfer **45**, 2087 (2002).